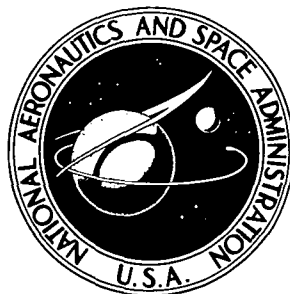


**NASA CONTRACTOR
REPORT**



N73-20913
NASA CR-2239

NASA CR-2239

**CASE FILE
COPY**

**LOAD INTERACTION EFFECTS
ON FATIGUE CRACK GROWTH
IN Ti-6Al-4V ALLOY**

by R. P. Wei, T. T. Shib, and J. H. FitzGerald

Prepared by

LEHIGH UNIVERSITY

Bethlehem, Pa.

for Langley Research Center

1. Report No. NASA CR-2239	2. Government Accession No.	3. Recipient's Catalog No.	
4. Title and Subtitle LOAD INTERACTION EFFECTS ON FATIGUE CRACK GROWTH IN Ti-6Al-4V ALLOY		5. Report Date April 1973	
		6. Performing Organization Code	
7. Author(s) R.P. WEI, T.T. SHIH, AND J.H. FITZGERALD		8. Performing Organization Report No. IFSM-72-15	
		10. Work Unit No. 501-22-02-01	
9. Performing Organization Name and Address DEPARTMENT OF MECHANICAL ENGINEERING AND MECHANICS LEHIGH UNIVERSITY BETHLEHEM, PENNSYLVANIA		11. Contract or Grant No. NGL 39-007-040	
		13. Type of Report and Period Covered CONTRACTOR REPORT	
12. Sponsoring Agency Name and Address NATIONAL AERONAUTICS AND SPACE ADMINISTRATION WASHINGTON, D.C. 20546		14. Sponsoring Agency Code	
15. Supplementary Notes			
16. Abstract THE IMPORTANCE OF DELAY, OR RETARDATION IN THE RATE OF FATIGUE CRACK GROWTH, PRODUCED BY LOAD INTERACTIONS IN VARIABLE AMPLITUDE LOADING, ON THE ACCURATE PREDICTION OF FATIGUE LIVES OF ENGINEERING STRUCTURES HAS BEEN WELL RECOGNIZED FOR SOME TIME. HERETOFORE, ONLY A FEW SIMPLE LOADING COMBINATIONS OR SPECTRA HAVE BEEN EXAMINED SYSTEMATICALLY. IN THIS INVESTIGATION THE EFFECTS OF A BROAD RANGE OF LOADING VARIABLES ON DELAY IN FATIGUE CRACK GROWTH AT ROOM TEMPERATURE ARE EXAMINED FOR A MILL ANNEALED Ti-6Al-4V ALLOY. THE RESULTS ARE USED TO ESTIMATE CRACK GROWTH BEHAVIOR UNDER PROGRAMMED LOADS. <i>Final Report</i>			
17. Key Words (Suggested by Author(s)) FATIGUE CRACK GROWTH VARIABLE-AMPLITUDE LOADING Ti-6Al-4V TITANIUM ALLOY LOAD INTERACTION EFFECTS		18. Distribution Statement UNCLASSIFIED - UNLIMITED	
19. Security Classif. (of this report) UNCLASSIFIED	20. Security Classif. (of this page) UNCLASSIFIED	21. No. of Pages 26	22. Price* \$3.00

Page Intentionally Left Blank

LOAD INTERACTION EFFECTS ON FATIGUE CRACK GROWTH IN Ti-6Al-4V ALLOY

R. P. Wei, T. T. Shih and J. H. FitzGerald
Department of Mechanical Engineering and Mechanics
LEHIGH UNIVERSITY
Bethlehem, Pennsylvania

SUMMARY

The importance of delay, or retardation in the rate of fatigue crack growth, produced by load interactions in variable amplitude loading, on the accurate prediction of fatigue lives of engineering structures has been well recognized for some time. Heretofore, only a few simple loading combinations or spectra have been examined systematically. In this investigation the effects of a broad range of loading variables on delay in fatigue crack growth at room temperature are examined for a mill annealed Ti-6Al-4V alloy. The results are used to estimate crack growth behavior under programmed loads.

INTRODUCTION

The importance of delay (or, retardation in the rate of fatigue crack growth) produced by load interactions in variable-amplitude loading, on the accurate prediction of fatigue lives and/or inspection intervals for engineering structures has been well recognized for some time [1-3]. Heretofore, only a few simple loading combinations or spectra have been examined systematically [3-5]. In a recent exploratory study, Jonáš and Wei [6] showed that the phenomenon of delay is very complex and can depend on a broad range of loading variables. This and other investigations have shown that the effects of delay can be quite large, and need to be taken into consideration in the development of improved analysis procedures for fatigue of engineering structures [6-8].

Several models have been proposed recently to account for the effects of delay [7,8]. These models, while successful in predicting trends in fatigue crack growth under randomized load spectra, break down for ordered spectra [7]. The lack of quantitative success may be attributed to:

- (a) a lack of physical and phenomenological understanding of the effects of load interactions on fatigue crack growth [4, 6-8], and of the simpler problem of fatigue crack growth itself; and,

- (b) inadequacies in stress analysis to account for the types of loading, crack geometry, and residual stresses [9-14].

To develop the needed understanding, a systematic examination of the effects of various loading variables on delay has been carried out in this investigation. Experiments were performed within the framework of linear elastic fracture mechanics. The crack tip stress intensity factor K or ΔK was used to characterize the mechanical crack driving force.

Delay properly refers to the period of abnormally low rate, or zero rate, of fatigue crack growth between a decrease in load level and the establishment of a rate of growth commensurate with that for constant amplitude loading at the prevailing (lower) load, that is, between points a and c in Figure 1. It is usually measured in terms of the number of elapsed load cycles. For experimental accuracy and potential engineering utility, however, it is more convenient to define delay N_D artificially as a period of zero crack growth, represented by a-b in Figure 1, which is obtained by extrapolating the constant-amplitude growth curve cd to b. Following Jonás^V and Wei [6], this definition for delay will be used here.

LIST OF SYMBOLS

a	crack length (half-crack length in center-cracked specimens)
$\Delta a/\Delta N$	rate of fatigue crack growth
K	stress intensity factor
K_{\max}	maximum value of K in one cycle
K_{\min}	minimum value of K in one cycle
$\Delta K = K_{\max} - K_{\min}$	stress intensity range
N	number of cycles
N_D	delay, in number of cycles (see Figure 1)
$R = K_{\min}/K_{\max}$	stress ratio
t	time at load
1, 2	subscripts 1 and 2 denote preloading (high load excursion) and subsequent loading conditions respectively

MATERIAL AND EXPERIMENTAL WORK

A 0.2-inch-thick (5.08 mm) mill annealed Ti-6Al-4V alloy plate was used in this investigation. The chemical composition, and longitudinal and transverse tensile properties of this alloy are given in Table 1. Constant load-amplitude fatigue crack growth data in several test environments are shown in Figure 2 for reference.

Three-inch-wide (76.2 mm) by 16-inch-long (406 mm) center-cracked specimens, oriented in the long transverse (TL) direction, were used in the fatigue crack growth studies. The initial center notch, about 0.4 inch (about 10 mm) long, was introduced by electro-discharge machining (EDM). The specimens were precracked in air at a stress ratio R of 0.05 through a sequence of loads that reduced ΔK to a level that is equal to or less than the selected starting ΔK level for the actual experiments. This precracking procedure provided fatigue cracks of about 0.08 inch (about 2 mm) in length from the ends of the starter notches, such that subsequent fatigue crack growth will be through material that has not been altered by the notch preparation procedure and will be unaffected by the starter notch geometry.

Delay experiments were carried out in air* under axial loading in a 100,000-lb. capacity MTS Systems closed-loop electro-hydraulic testing machine operated principally at 5 Hz. Deviations from this loading frequency were made when a single or a small number of high load cycles were to be applied, and when extremely long delays were experienced. Load control was estimated to be better than ± 1 percent. A continuous-recording electrical potential system was used for monitoring crack growth [15,16]. Using a working current of about 2.1 amperes, this system provided an average measurement sensitivity of about 0.0025 inch (0.064 mm) in half-crack length, a, per microvolt (μv) change in potential (that is, 0.0025 in./ μv or 0.064 mm/ μv) for these specimens. Resolution was better than 0.0015 inch (0.038 mm). The electrical potential method provides measurements of the average crack length (through the

* Comparison experiments indicated that delay in air was not significantly different from that obtained in a dehumidified argon environment. For convenience, therefore, all delay experiments were carried out in air. Aggressive environments, such as salt water, and test temperature, however, have significant effects on delay. These effects will be discussed in a separate paper.

thickness), as opposed to the visual methods which give measurements of the crack length at the specimen surface only. Hence, this method can detect the onset of crack growth from the mid-thickness region of the specimens, that is, crack tunneling.

Because previous experiments [6] indicated the existence of a significant effect on delay when a high load excursion occurred during delay produced by a previous high load excursion, a series of experiments was conducted to establish proper test conditions for this investigation. The results of these experiments are shown in Figure 3. For example, a single high load excursion to $28 \text{ ksi-in}^{\frac{1}{2}}$ followed by cycling at a ΔK_2 of $14 \text{ ksi-in}^{\frac{1}{2}}$ resulted in a delay, N_D , of about 7,000 cycles. The introduction of a second high load excursion of the same magnitude immediately after the first excursion increased N_D by about 4,000 cycles to about 11,000 cycles. By increasing the interval between the high load excursions, N_D is increased by lesser amounts, and returns to that of a single high load excursion after the crack had been extended by about 0.085 inch (2.16 mm) between the successive high load excursions, Figure 3. Such a procedure was utilized in this investigation, and permitted an average of five individual delay experiments to be performed on each test specimen.

RESULTS AND DISCUSSIONS

In an exploratory investigation, Jonáš^v and Wei [6] found that delay, N_D , was a function of ΔK_1 , ΔK_2 (or $\Delta K_1/\Delta K_2$), R_1 , N_1 and t_1 , where the subscripts 1 and 2 denote preloading and the subsequent loading conditions respectively. ΔK is the stress intensity range for a given loading cycle (that is $\Delta K = K_{\max} - K_{\min}$); $R = K_{\min}/K_{\max}$; N = the number of load cycles; and t = time at load.

$$N_D = F [\Delta K_1, \Delta K_2 \text{ (or } \Delta K_1/\Delta K_2), R_1, R_2, N_1, t_1]$$

Other studies showed that delay depends also on the test temperatures T_1 and T_2 , and on the test environment. The effects of these environmental variables will be discussed in a separate paper. In this investigation, a more systematic examination of the influences of ΔK_1 , ΔK_2 , R_1 , R_2 and N_1 was made. For the sake of completeness, the results of the exploratory study are included in Figure 4, and will be discussed along with the results from this investigation.

The effects of a broad range of loading variables are shown in Figures 4 to 11, and may be summarized below:

1. Comparison of Figures 4(a) and 4(b) shows that relaxation at zero load following a high load excursion decreases delay [6].
2. Comparisons between Figures 4(b), 4(c) and 4(d), and between Figures 4(g) and 4(h) show that holding at high load increases delay. Delay is increased with increasing time at load, t_1 [6].
3. Comparison of Figure 4(f) with Figure 4(g) shows that delay is a minimum when compression loading is applied following a high load excursion [6].
4. For fixed values of ΔK_2 (or ΔK_1), delay depends strongly on ΔK_1 (or ΔK_2) or on the ratio between ΔK_1 and ΔK_2 , Figure 5. This effect can be very large. For example, loading at a ΔK_2 of about $10 \text{ ksi-in}^{\frac{1}{2}}$ ($11 \text{ MN-m}^{-3/2}$) (with $R \approx 0$), following a single high load excursion to $28 \text{ ksi-in}^{\frac{1}{2}}$ ($30.8 \text{ MN-m}^{-3/2}$), (that is, $\Delta K_1/\Delta K_2 = 2.8$), produced no detectable crack growth after 450,000 cycles, indicating a delay of much greater than 450,000 cycles, Figure 5(b). (The normal rate of fatigue crack growth under this condition would have been of the order of 10^{-6} inch per cycle.)
5. By increasing ΔK_2 to $14 \text{ ksi-in}^{\frac{1}{2}}$ ($15.4 \text{ MN-m}^{-3/2}$) after 450,000 cycles at a ΔK_2 of $10 \text{ ksi-in}^{\frac{1}{2}}$ ($11 \text{ MN-m}^{-3/2}$), (in the loading sequence described in item 4 above), a delay of 6,500 cycles was observed. This delay is consistent with those obtained for a direct change in loading from 28 to $14 \text{ ksi-in}^{\frac{1}{2}}$ (30.8 to $15.4 \text{ MN-m}^{-3/2}$), Figure 5(a). This result suggests that delay is substantially unaffected by intermediate cyclic loading during which no crack growth takes place.
6. For a constant value of $\Delta K_1/\Delta K_2$, delay decreases with increasing ΔK_2 , Figures 6 and 7.
7. For fixed values of ΔK_1 and ΔK_2 , delay decreases with increasing R_2 , and coincidentally with increasing values of $K_{2\text{max}}/K_{1\text{max}}$. When $K_{2\text{max}}$ is equal to (or exceeds) $K_{1\text{max}}$, no delay will be experienced, Figures 8 and 9.
8. When a high load excursion occurs during delay produced by a previous high load excursion, the resulting delay appears to depend on the interval, or

extent of crack growth, between the high load excursions, Figures 2 and 4. Delay is increased by the proximity to the first high load excursion and decreases with crack extension between the high load excursions. The extent of crack growth required to eliminate the effect of the first high load excursion appears to be an order of magnitude larger than the crack tip plastic zone size, r_{y1} , Figure 2, and is expected to be dependent on the test temperature and loading history.

9. Delay increases with the number of repeated high load excursions, N_1 , Figure 10. Unlike the results of Hudson and Raju [4], however, it reaches a maximum and then decreases with increasing N_1 . The results suggest that this maximum may be dependent on R_1 , among other possible variables.
10. The effect of R_1 was not examined specifically. By cross plotting available data, however, it may be seen that delay is strongly affected by R_1 also, Figure 11. The behavior appears to be more complex and to be dependent on the number of high load cycles.

It is clear that delay in fatigue crack growth caused by load interactions is a highly complex phenomenon. No satisfactory model has been developed to account for all of the observed behavior [7, 8]. The results of this investigation suggest that residual stress at the crack tip would play an important role in delaying crack growth. Observation on an interrupted test* indicates that the reinitiation of fatigue crack growth, following a high load excursion, proceeds from the mid-thickness region of a specimen, Figure 12. This observation suggests that delay is caused primarily by residual stresses introduced by plastic deformation at the specimen surface, and that delay, in essence, is a three dimensional problem.

To examine the implications of delay on fatigue crack growth under variable-amplitude loading, experiments were carried out using simple block programming. A simple 4-layer (or, 4 load level) block spectrum was used. Loads were selected to give ΔK levels of approximately 12, 16, 20 and 24 $\text{ksi-in}^{\frac{1}{2}}$ (13.2, 17.6, 22 and 26.4 $\text{MN-m}^{-3/2}$); with $R = 0$ and with 6,000, 1,200, 600 and 300 cycles in the respective layers. Both a

* Tested in air at 560°F.

low-to-high and a high-to-low sequence were examined. Cumulative crack growth after each layer for each of the spectra is given in Table 2. These results are compared with estimates computed on the basis of the definition of delay (Figure 1) and the delay and crack growth data (Figures 2 to 11). (The estimation procedure is given in the Appendix). It is seen that the spectrum load data are consistent with the estimated results, and therefore consistent with the delay data (although the close agreement indicated in Table 2 may be somewhat fortuitous, it is representative of the general behavior). In the low-to-high sequence, there is no delay in the first load block since the loads appeared in ascending order. In the first layer of the second block, and of subsequent blocks, nearly no crack growth took place because of delay. Some crack growth occurred in the second layer of the second and subsequent load blocks, since the number of applied cycles was larger than the delay. Because of growth in the second layer, little or no delay would be expected in the third layer; and no delay occurred in the fourth and final layer in each block. In the high-to-low sequence, on the other hand, no delay occurred in the first (highest load) layer in each block. Delay and some crack growth occurred in each of the succeeding layers, such that delay in each layer is affected only by the previous layer. Because of these differences, a sequence effect occurred, such as those reported in the literature [7].

CONCLUSION

A phenomenological examination of delay, or retardation in the rate of fatigue crack growth, produced by load interactions was made. The delay phenomenon was found to be very complex and to be strongly dependent on all of the loading variables, such as stress intensity range, stress ratio, number of cycles of high load, time at high load, etc. Estimates based on the phenomenological data on delay indicate the presence of a sequence effect for programmed loading. These estimates are consistent with experimental observations. These results suggest that a consistent phenomenological model for estimating fatigue crack growth under variable-amplitude loading can be developed.

APPENDIX

Procedure for Estimating Crack Growth under Programmed Loading

A numerical integration procedure was used for estimating fatigue crack growth under programmed loading. This procedure utilized piece-wise power law representations of the constant load-amplitude fatigue crack growth data, and delay data from the experimental program. A power law of the following form was used:

$$\frac{\Delta a}{\Delta N} = A (\Delta K)^n \quad (A-1)$$

where A and n are empirical constants. For $\Delta a/\Delta N$ and ΔK to be expressed in units of in./cycle and ksi-in^{1/2} respectively, the empirical constant A assumes the dimension of (in./cycle) (ksi-in^{1/2})⁻ⁿ. The following values of A and n were used (air data from Figure 2, with R ≈ 0):

$$\begin{aligned} \text{For } \Delta K < 14 \text{ ksi-in}^{\frac{1}{2}} \quad n = 3.6 \quad A = 3.38 \times 10^{-10} (\text{in./cycle}) (\text{ksi-in}^{\frac{1}{2}})^{-3.6} \\ \text{For } \Delta K \geq 14 \text{ ksi-in}^{\frac{1}{2}} \quad n = 2.6 \quad A = 5.18 \times 10^{-9} (\text{in./cycle}) (\text{ksi-in}^{\frac{1}{2}})^{-2.6} \end{aligned}$$

Delay data for a single high load excursion was estimated from Figures 5-7, and are shown in Figure A-1. (Approximate adjustments were made to account for multiple high load excursions as required.) Procedurally, delay encountered in the ith load layer, N_{Di}, was estimated on the basis of ΔK at the start of the ith layer, ΔK_i , and ΔK at the end of the previous layer, $\Delta K_{(i-1)}$. The increment of crack growth during the ith layer was determined numerically by integrating Equation A-1 between N_{Di} and N_i, where N_i = total number of cycles in the ith layer. Integration was performed only when N_i exceeded N_{Di}. If no crack growth took place during the (i - 1)th layer, N_{Di} was estimated on the basis of the next previous layer, that is, the (i - 2) layer. A more detailed discussion of the steps used in obtaining the results in Table 2 is given below.

Two indices j - k were used to designate the load-block (j) and load-layer (k) in the block programmed load used in Table 2. In the low-to-high sequence, no delay would be encountered in the 1-1, 1-2, 1-3 and 1-4 layers, since the loads appeared in ascending order. Cumulative crack growth was calculated straight-forwardly from Equation A-1. For the 2-1 and 3-1 layers, delay was estimated to be about 12,000 cycles.

This value was estimated from Figure A-1 for a single high load excursion, and was adjusted approximately for multiple high load excursions on the basis of Figure 10 by proportion. Since the delay was larger than the number of applied load cycles in these layers, no crack growth was obtained. Since crack growth did not take place during the 2-1 and 3-1 layers, estimates for delay in the 2-2 and 3-2 layers were based on comparisons of ΔK levels in the 1-4 and 2-2, and 2-4 and 3-2 layers respectively. Delay in these layers was estimated to be about 1,000 cycles. Because of the delay, crack growth was assumed to be zero during the first 1,000 cycles in these layers. Crack growth during the remaining 200 cycles was then calculated by integration of Equation A-1. Because of crack growth in the 2-2 and 3-2 layers, the high loads in the 1-4 and 2-4 layers were assumed to exert no further influence on the subsequent layers, that is, the 2-3 and 2-4, and 3-3 and 3-4 layers, respectively. Crack growth in each layer was then calculated straight-forwardly. Crack growth for the high-to-low sequence was estimated in a similar manner.

REFERENCES

1. R. H. Christensen, Proceedings - Crack Propagation Symposium, Cranfield, College of Aeronautics, (1962).
2. J. Schijve, Fatigue Crack Propagation in Light Alloy Sheet Material and Structures, Rept. MP 195, National Luchtvaartlaboratorium (Amsterdam), (August 1960).
3. C. M. Hudson and H. F. Hardrath, NASA TN D-960, (1961).
4. C. M. Hudson and K. N. Raju, NASA TN D-5702, (1970).
5. J. P. Butler, "The Material Selection and Structural Development Process for Aircraft Structural Integrity under Fatigue Conditions," AFFDL TR-70-144 (1970), 17.
6. O. Jonás^{IV} and R. P. Wei, Int'l. J. Fract. Mech., 7 (1971), 116-118.
7. O. E. Wheeler, "Spectrum Loading and Crack Growth," ASME Paper No. 71-Met-X, (1971).
8. W. Elber, "The Significance of Crack Closure," presented at the 1970 Annual Meeting of ASTM, Toronto, Canada (21-26, June 1970).
9. W. F. Brown, Jr. and J. E. Srawley, ASTM STP 410 (1966).
10. P. C. Paris and G. C. Sih, ASTM STP 381 (1965).
11. G. C. Sih, Int'l. J. Fract. Mech., 7, 39-61 (1971).
12. R. J. Hartranft and G. C. Sih, J. Math. Mechanics, 19 (1969), 123.
13. F. W. Smith, A. F. Emery and A. S. Kobayashi, J. Appl. Mech., 34 (1967), 953.
14. G. R. Irwin, J. Appl. Mech., 29 (1962), 651.
15. H. H. Johnson, Mat. Res. and Stds., 4, ASTM (1965), 442.
16. Che-Yu Li and R. P. Wei, Mat. Res. and Std., 6, ASTM (1966), 392.
17. R. P. Wei and D. L. Ritter, "The Influence of Temperature on Fatigue-Crack Growth in a Mill Annealed Ti-6Al-4V Alloy," J. of Mat'ls., 7, ASTM (1972), 240.

TABLE 1

Chemical Composition and Tensile Properties
(Reactive Metal Ingot No. 293831, Lot 05)

Chemical Composition - Weight Percent
(Ingot Analysis)

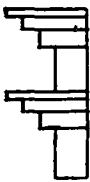

<u>C</u>	<u>N</u>	<u>Fe</u>	<u>Al</u>	<u>V</u>	<u>O</u>	<u>H (ppm)</u>	<u>Ti</u>
0.03	0.013	0.13	6.2	4.2	0.12	90	Balance

Tensile Properties*

<u>Direction</u>	<u>Yield Strength</u> <u>ksi (MN/m²)</u>	<u>Tensile</u> <u>Strength</u> <u>ksi (MN/m²)</u>	<u>Elongation</u> <u>in 2 in.</u> <u>percent</u>
Transverse			
	149.5 (1,031)	152.6 (1,052)	12.5
	149.8 (1,033)	153.4 (1,058)	12.5
	<u>148.3 (1,023)</u>	<u>151.4 (1,044)</u>	<u>11.7</u>
(Average)	149.2 (1,029)	152.5 (1,051)	12.2
Longitudinal			
	-----	150.7 (1,039)	11.7
	141.1 (973)	151.0 (1,041)	11.7
	<u>141.9 (978)</u>	<u>151.8 (1,047)</u>	<u>12.5</u>
(Average)	141.5 (976)	151.2 (1,042)	12.0

* Production annealed 1,450°F, 15 min. + air cool.

Table 2: Comparison of Estimated and Measured Crack Growth under Block Programmed Loads ($R = 0$; $f = 5.0$ Hz) in Air at Room Temperature

Sequence	Block No.	Layer No.	Load* (lbs)	No. of Cycles	Est. Delay (Cycles)	Cumulative Crack Growth (in.)**	
						Measured	Estimated
Low-High ($a_o = 0.6019$) 	1	1	5,220	6,000	0	(Not Included)	---
		2	6,960	1,200	0	0.0077	0.009
		3	8,700	600	0	0.0155	0.018
		4	10,420	300	0	0.0227	0.024
	2	1	5,220	6,000	12,000	0.0230	0.024
		2	6,960	1,200	1,000	0.0248	0.026
		3	8,700	600	0	0.0323	0.035
		4	10,420	300	0	0.0398	0.042
	3	1	5,220	6,000	12,000	0.0399	0.042
		2	6,960	1,200	1,000	0.0421	0.044
		3	8,700	600	0	0.0503	0.053
		4	10,420	300	0	0.0582	0.061
High-Low ($a_o = 0.7414$) 	1	1	8,800	300	0	0.0061	0.006
		2	7,330	600	150	0.0118	0.012
		3	5,870	1,200	500	0.0173	0.017
		4	4,400	6,000	1,500	0.0303	0.031
	2	1	8,800	300	0	0.0371	0.038
		2	7,330	600	150	0.0434	0.044
		3	5,870	1,200	500	0.0499	0.050
		4	4,400	6,000	1,500	0.0643	0.065
	3	1	8,800	300	0	0.0724	0.073
		2	7,330	600	150	0.0794	0.080
		3	5,870	1,200	500	0.0865	0.087
		4	4,400	6,000	1,500	0.1024	0.105

* 1 lb. \approx 4.448 N

** 1 in. = 2.54×10^{-2} m

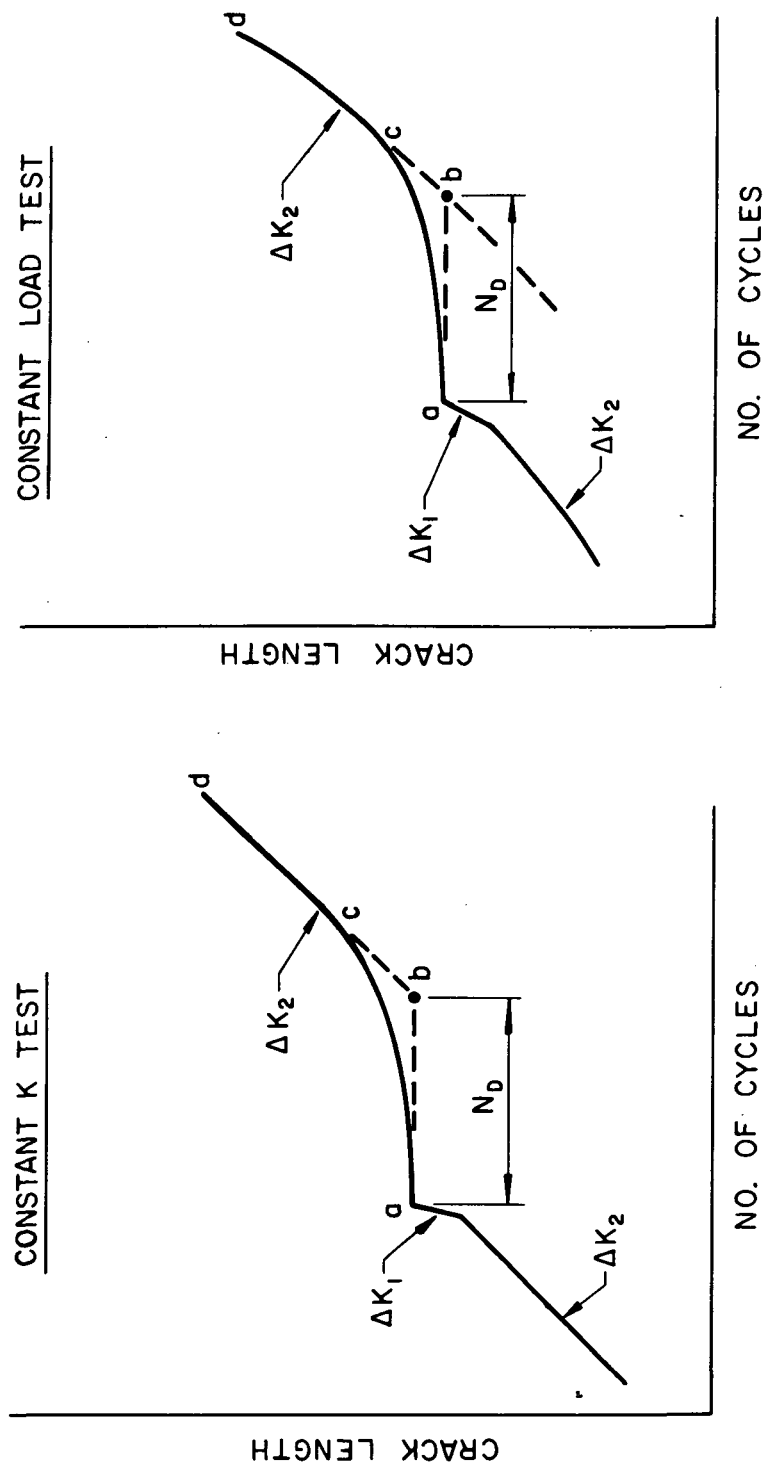


Figure 1: Schematic Illustration of Delay in Fatigue Crack Growth and Definition of N_D [6].

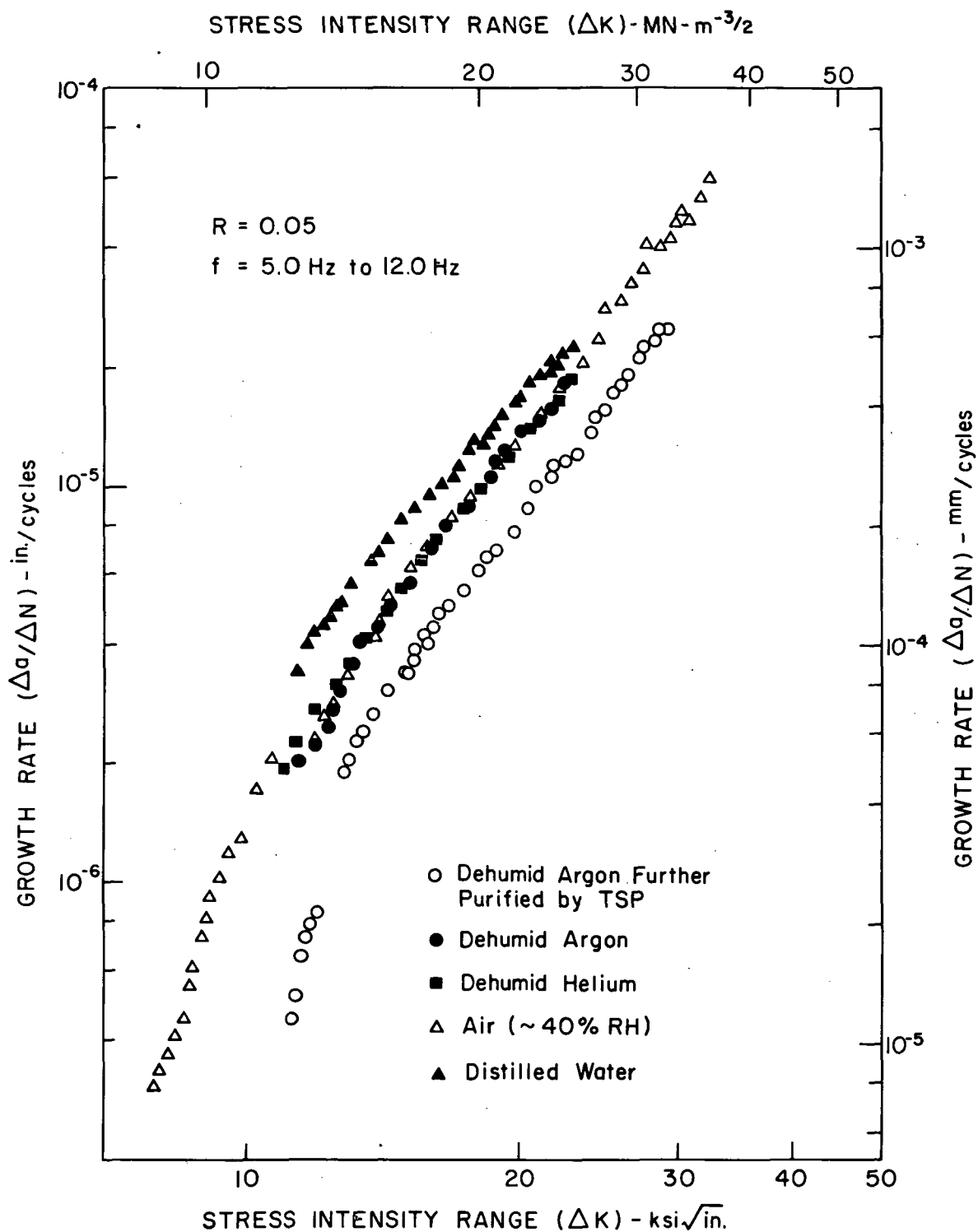


Figure 2: Kinetics of Fatigue Crack Growth in Various Environments at Room Temperature. (Residual moisture in the dehumidified environments were well below 30 ppm [17]).

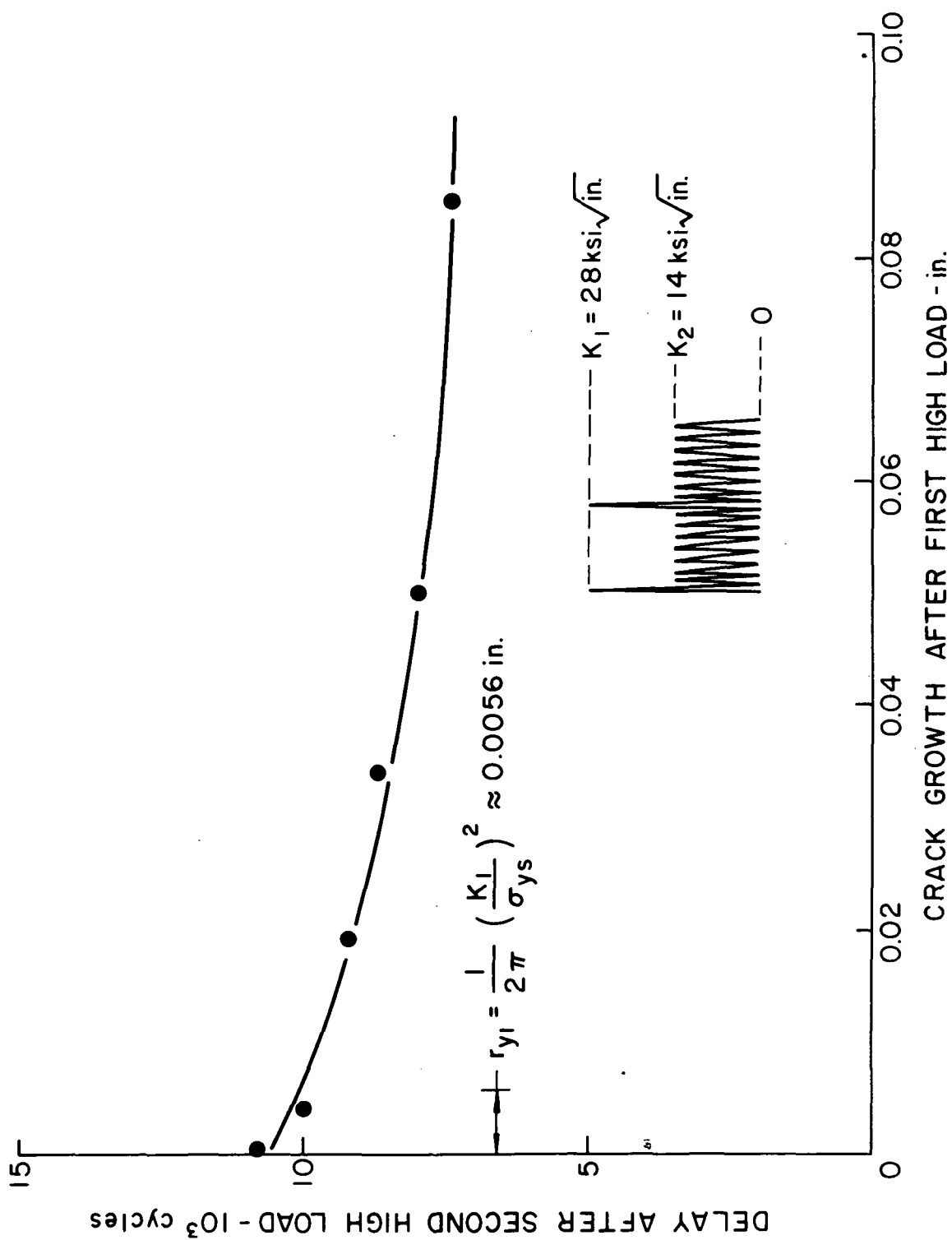


Figure 3: Effect of Crack Growth between Consecutive High Load Excursions on the Subsequent Delay.

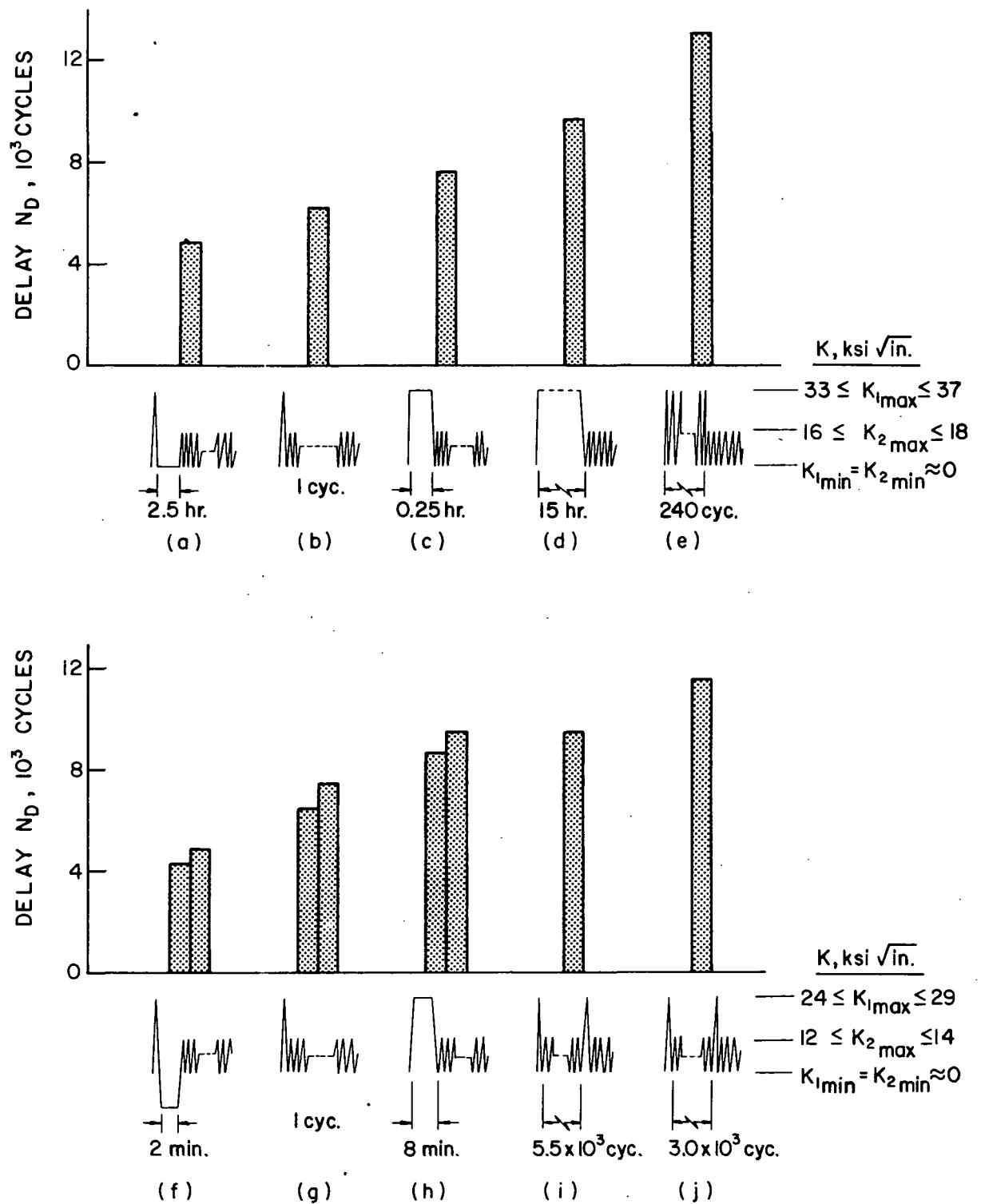


Figure 4: Delay in Fatigue Crack Growth Produced by Various Simple Load Sequences [6]. (Each bar represents an individual data point).

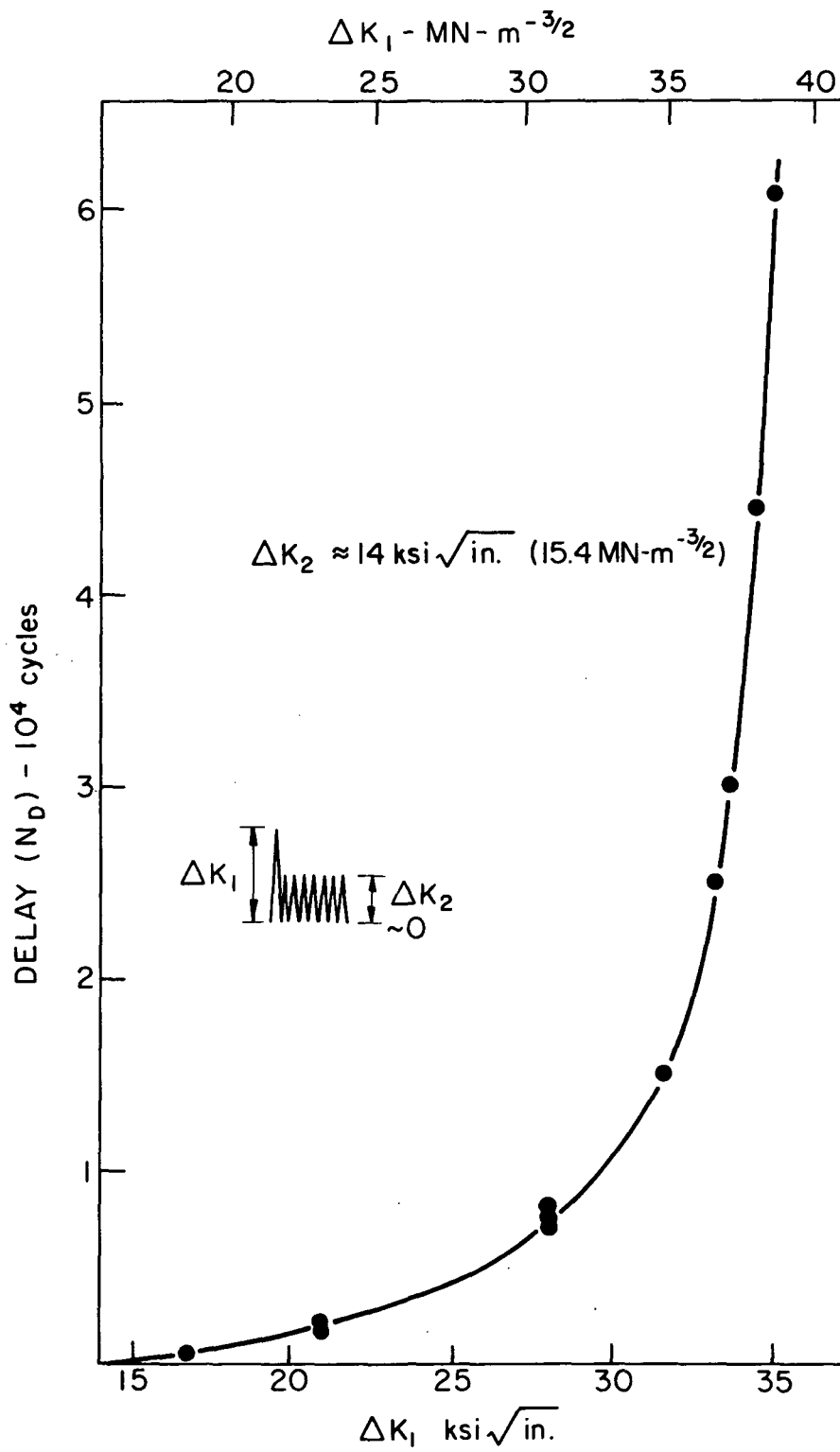


Figure 5a: Effect of ΔK_I on Delay

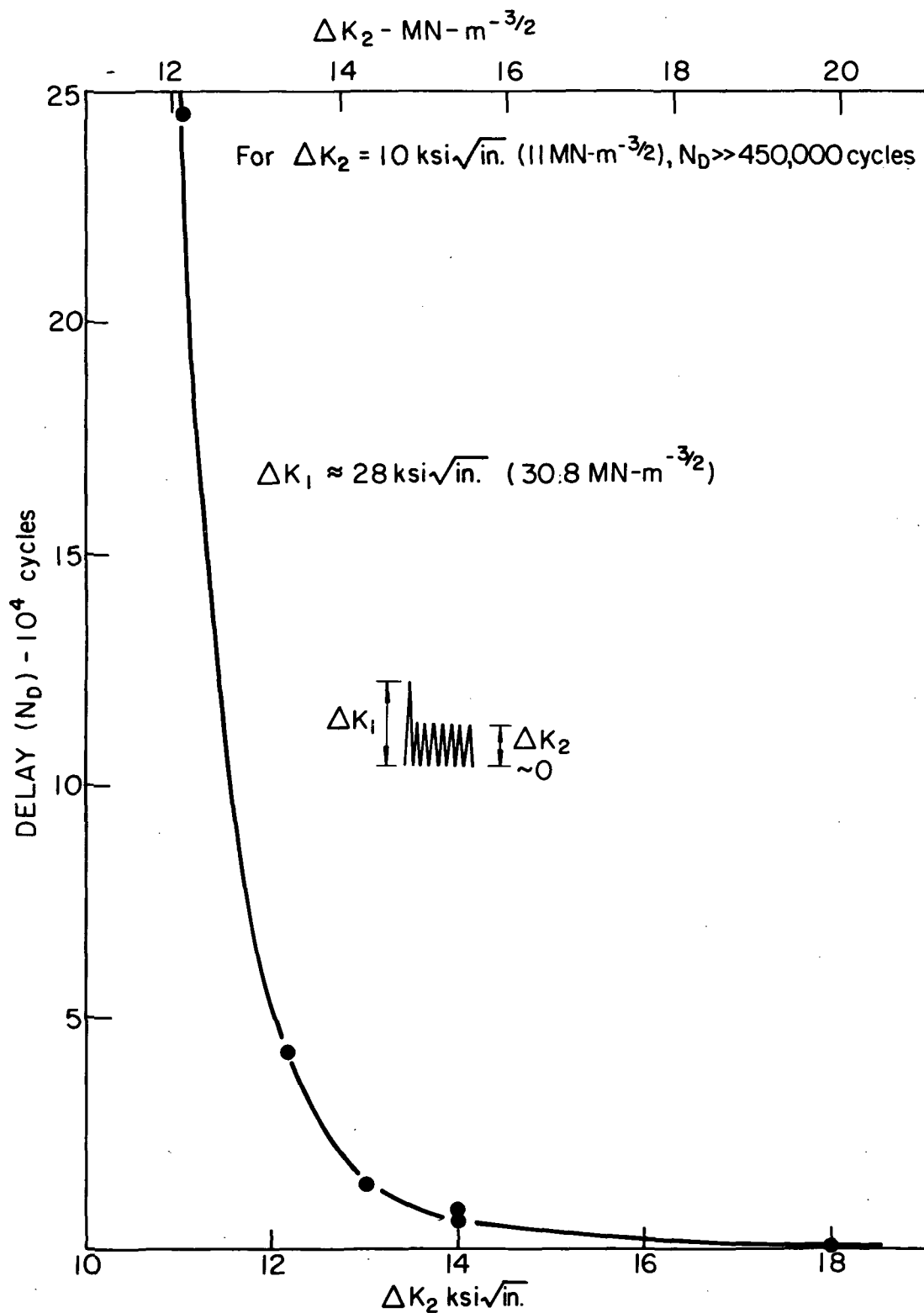


Figure 5b: Effect of ΔK_2 on Delay

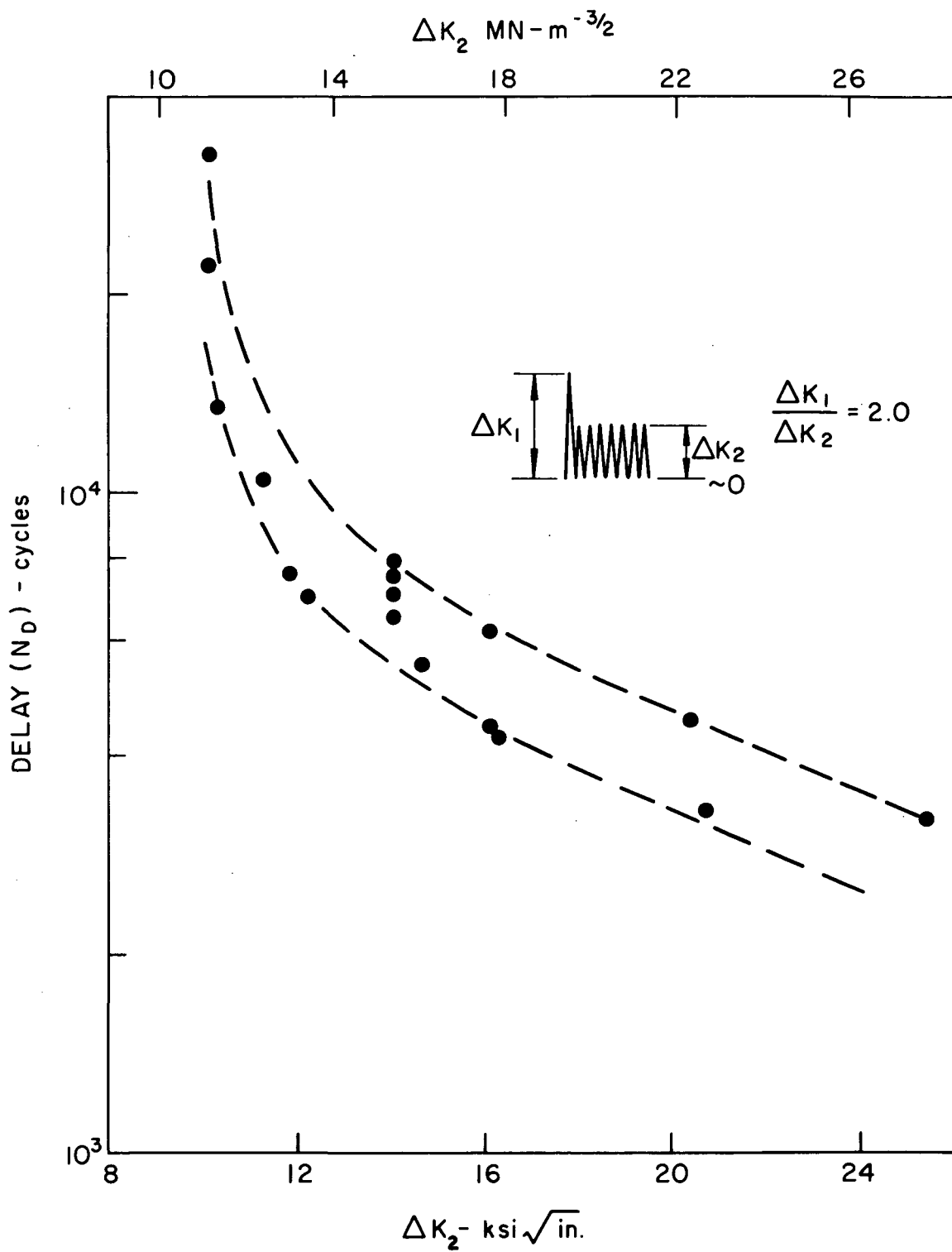


Figure 6: Effect of ΔK_2 on Delay for $\Delta K_1 / \Delta K_2 = 2.0$.

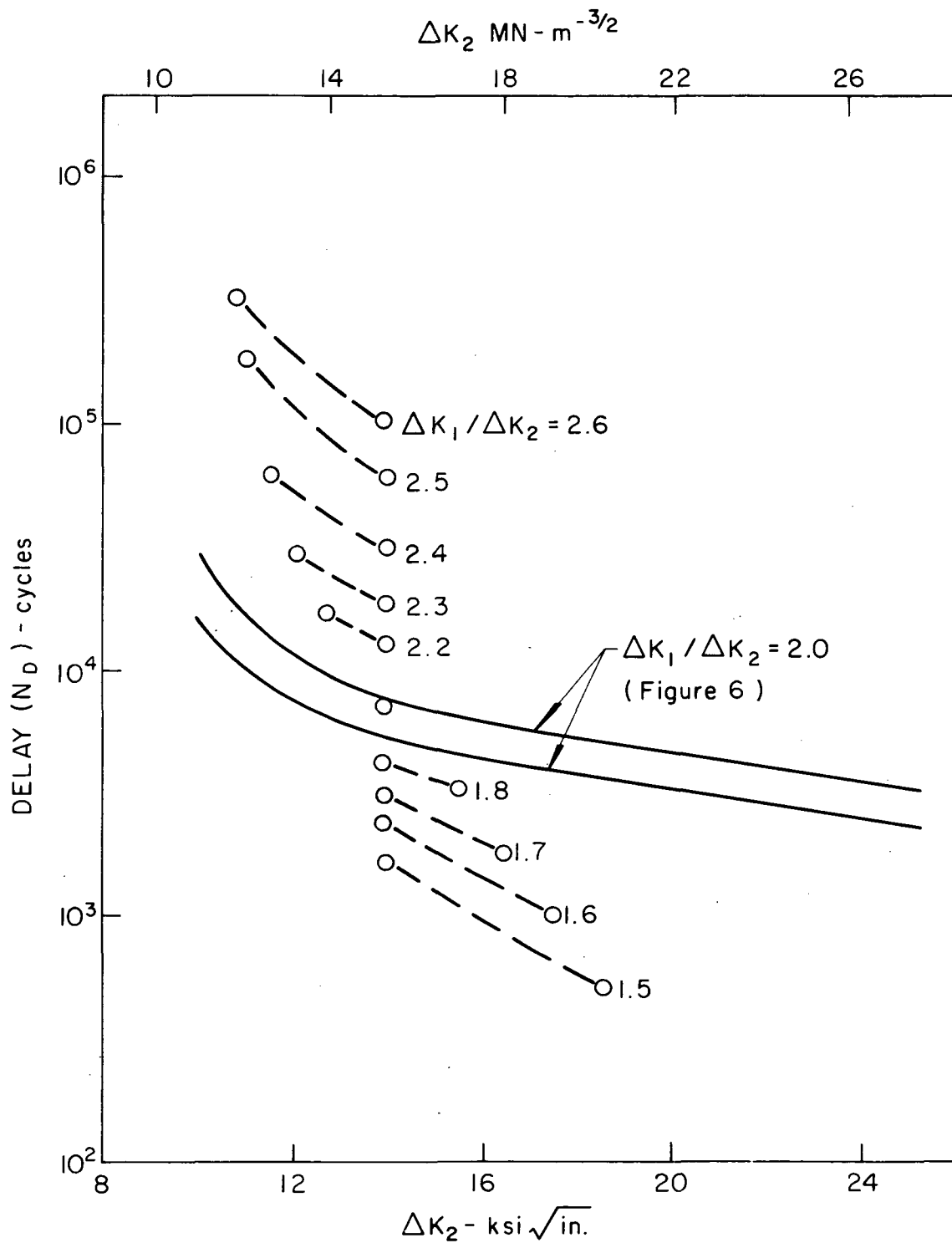


Figure 7: Effect of ΔK_2 on Delay for Constant $\Delta K_1 / \Delta K_2$.

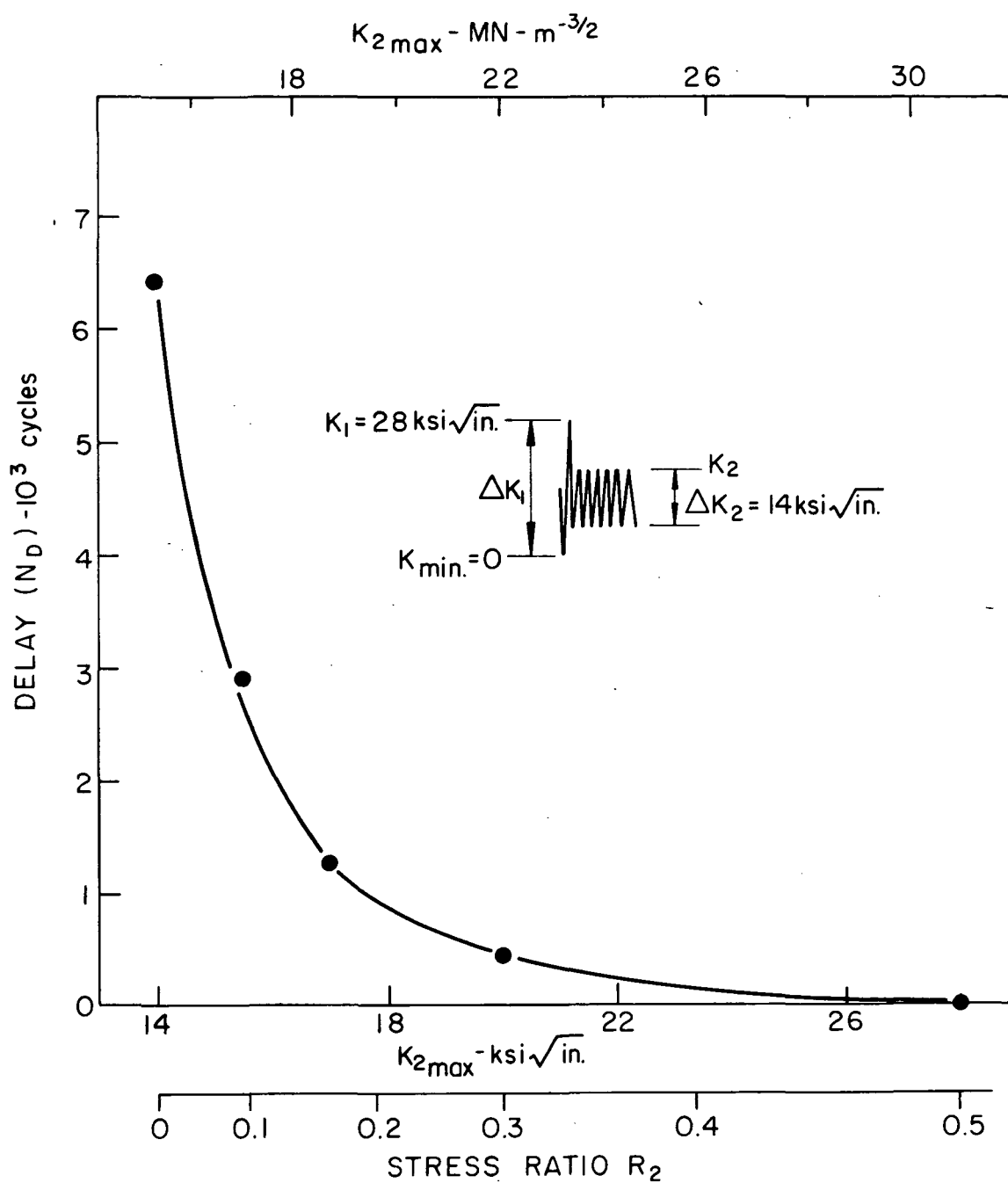


Figure 8: Effect of R_2 or $K_{2\max}$ on Delay.

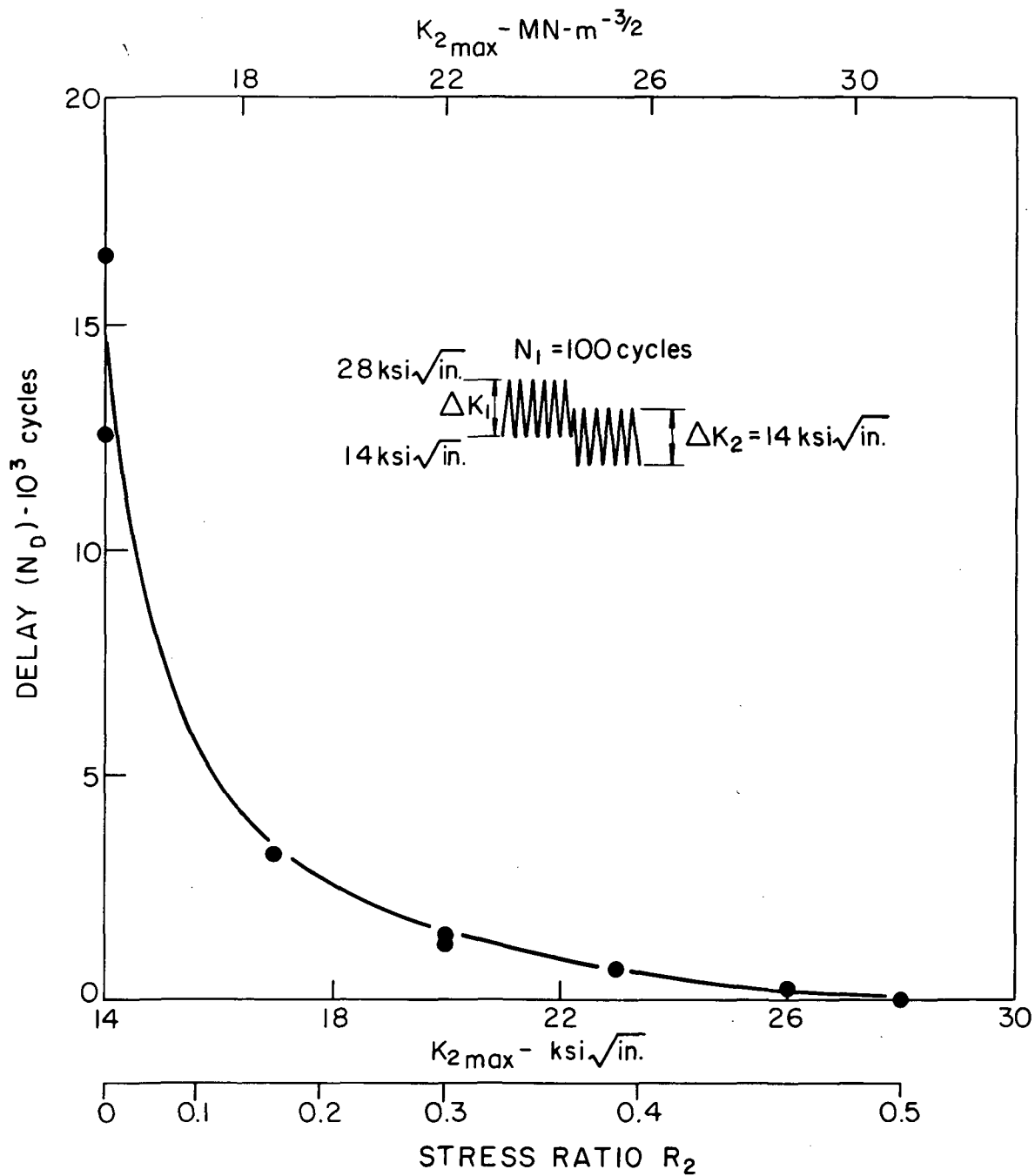


Figure 9: Effect of R_2 or $K_{2\max}$ on Delay.

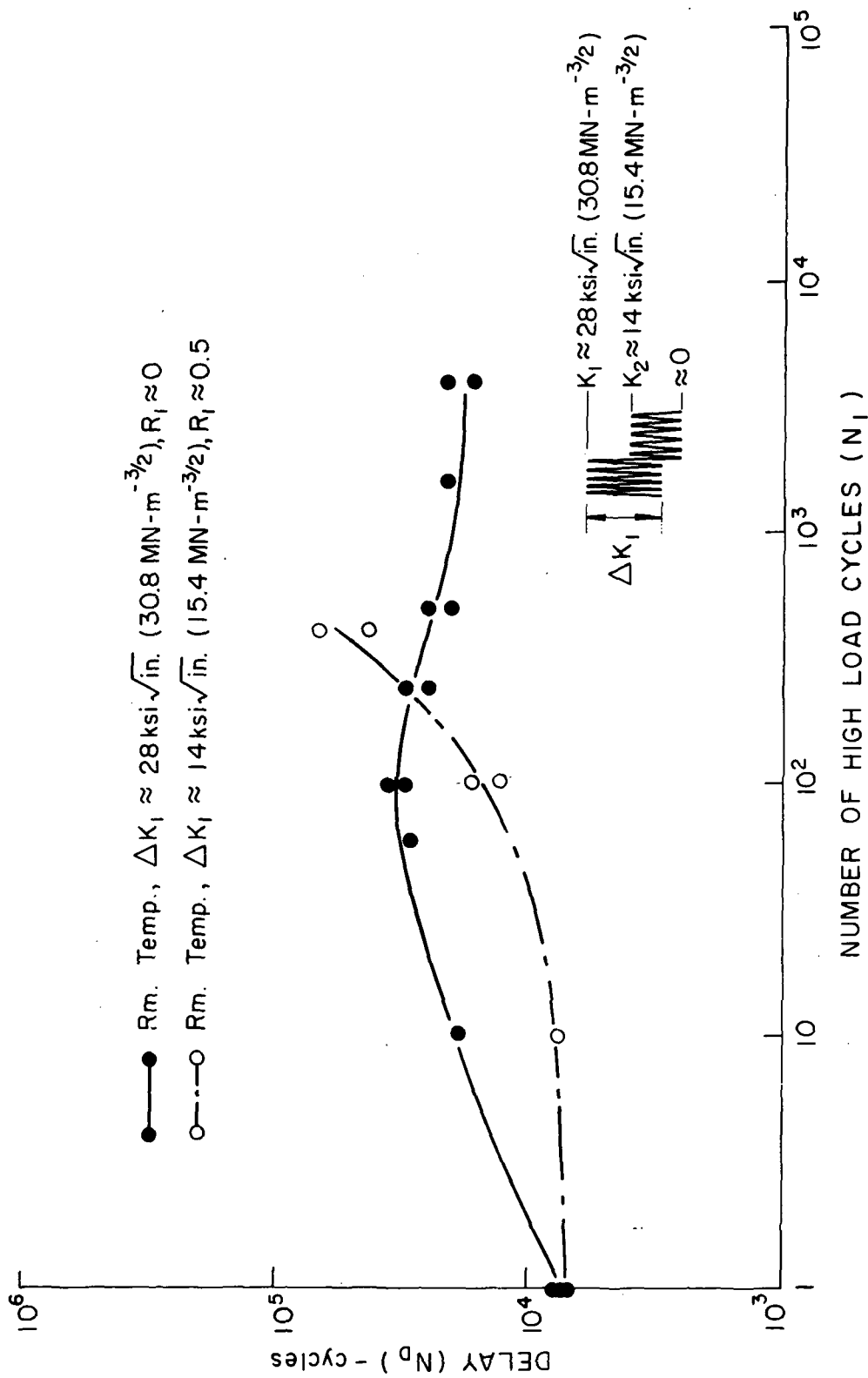


Figure 10: Effect of Multiple High Load Excursions on Delay.

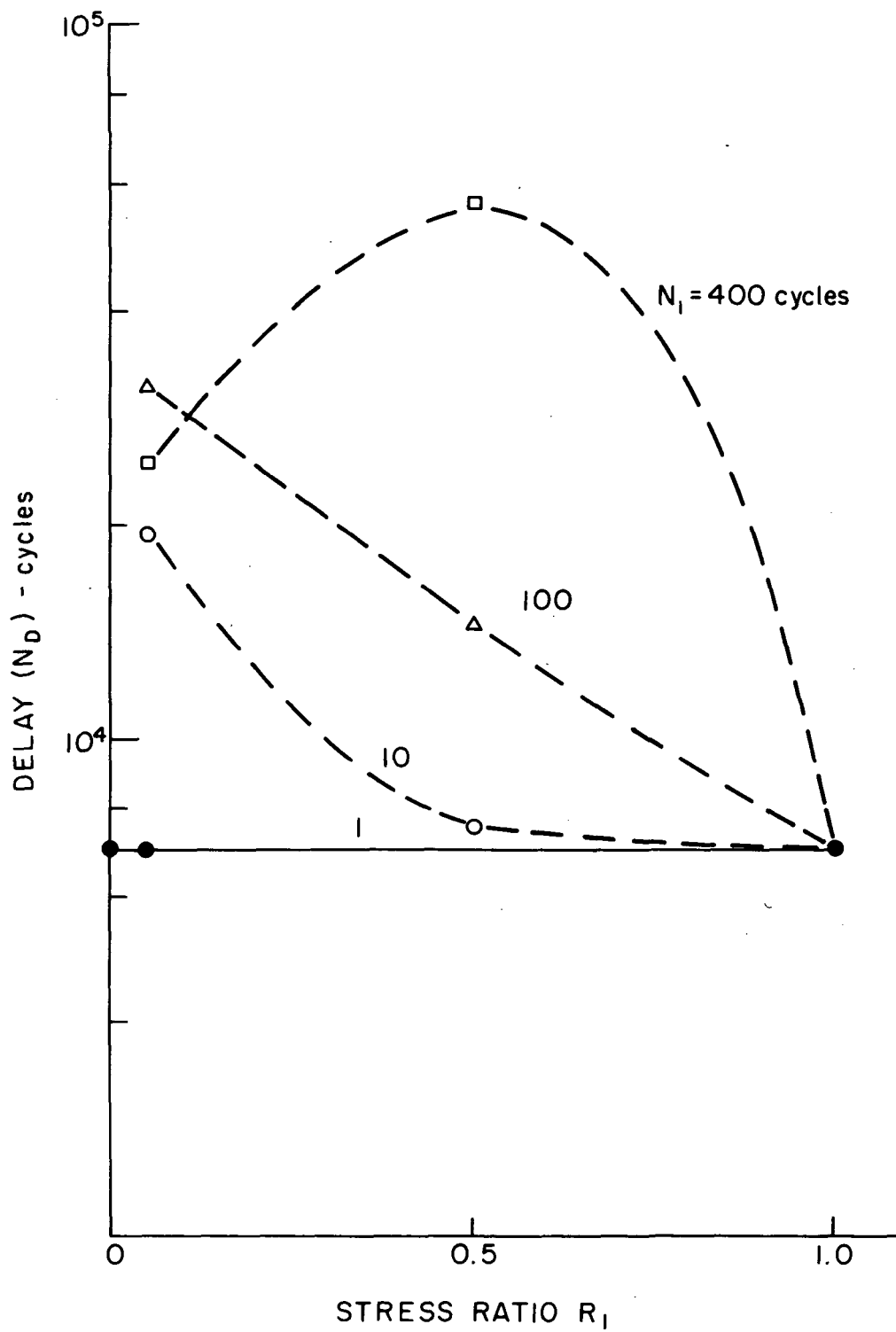


Figure 11: Effects of R_1 and N_1 on Delay.

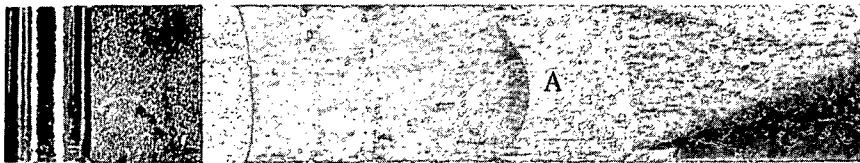


Figure 12: Macrofractograph Showing Onset of Crack Growth from the Mid-Thickness Region Following a High Load Excursion at A.

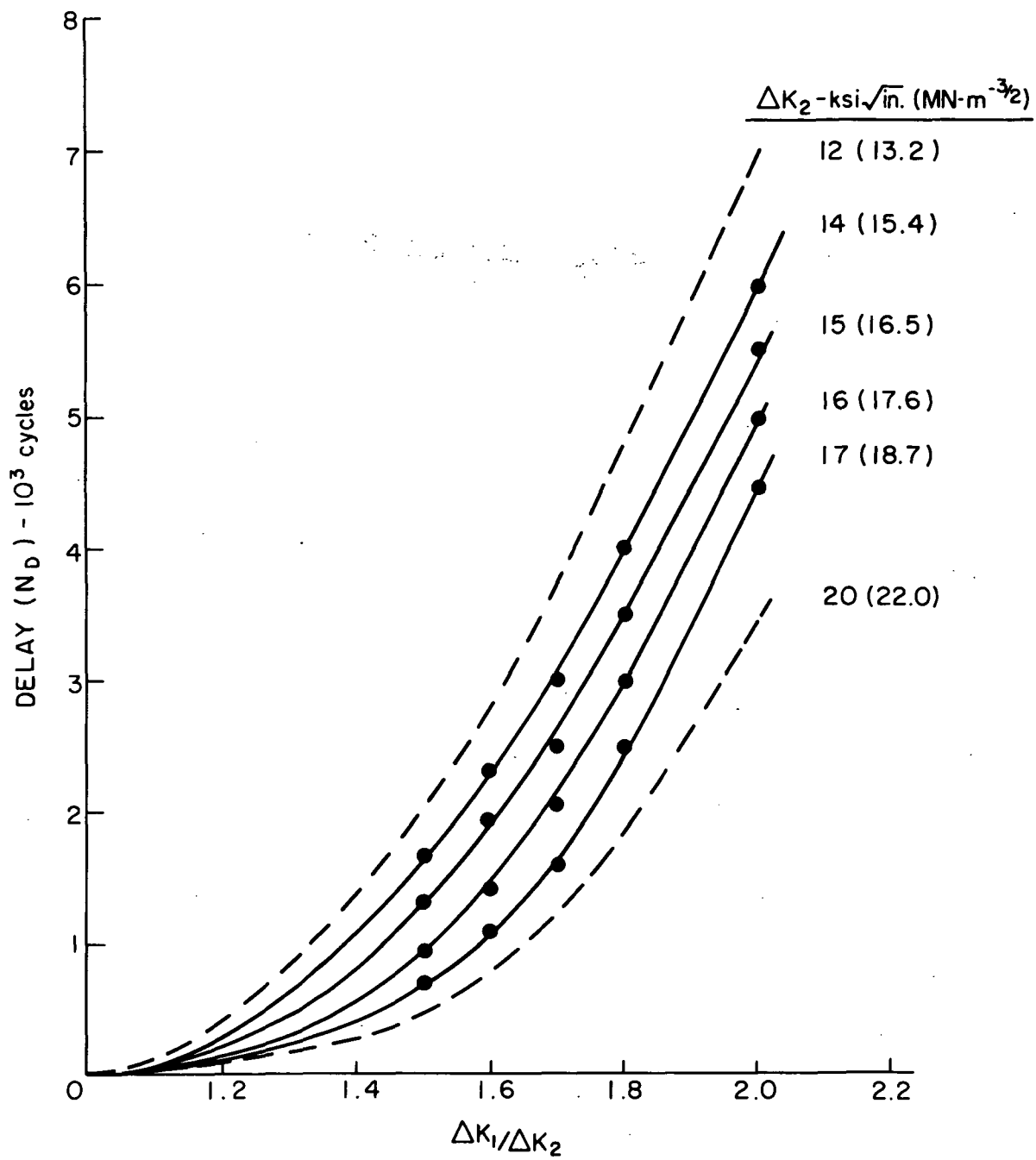


Figure A-1: Effect of $\Delta K_1 / \Delta K_2$ on Delay.

Page Intentionally Left Blank



POSTMASTER : If Undeliverable (Section 158
Postal Manual) Do Not Return

"The aeronautical and space activities of the United States shall be conducted so as to contribute . . . to the expansion of human knowledge of phenomena in the atmosphere and space. The Administration shall provide for the widest practicable and appropriate dissemination of information concerning its activities and the results thereof."

—NATIONAL AERONAUTICS AND SPACE ACT OF 1958

NASA SCIENTIFIC AND TECHNICAL PUBLICATIONS

TECHNICAL REPORTS: Scientific and technical information considered important, complete, and a lasting contribution to existing knowledge.

TECHNICAL NOTES: Information less broad in scope but nevertheless of importance as a contribution to existing knowledge.

TECHNICAL MEMORANDUMS: Information receiving limited distribution because of preliminary data, security classification, or other reasons. Also includes conference proceedings with either limited or unlimited distribution.

CONTRACTOR REPORTS: Scientific and technical information generated under a NASA contract or grant and considered an important contribution to existing knowledge.

TECHNICAL TRANSLATIONS: Information published in a foreign language considered to merit NASA distribution in English.

SPECIAL PUBLICATIONS: Information derived from or of value to NASA activities. Publications include final reports of major projects, monographs, data compilations, handbooks, sourcebooks, and special bibliographies.

TECHNOLOGY UTILIZATION PUBLICATIONS: Information on technology used by NASA that may be of particular interest in commercial and other non-aerospace applications. Publications include Tech Briefs, Technology Utilization Reports and Technology Surveys.

Details on the availability of these publications may be obtained from:

SCIENTIFIC AND TECHNICAL INFORMATION OFFICE

NATIONAL AERONAUTICS AND SPACE ADMINISTRATION

Washington, D.C. 20546